Syntheses and Properties of Dimethyl and Tetramethyl Anthra[1,9-*cd*:4,10-*c'd'*]-bis[1,2]dichalcogenoles and Their Charge-Transfer Complexes

Kazuo TAKIMIYA, Yoshio ASO, Tetsuo OTSUBO, and Fumio OGURA*
Department of Applied Chemistry, Faculty of Engineering, Hiroshima University, Kagamiyama, Higashi-Hiroshima 724
(Received February 18, 1991)

The dimethyl and tetramethyl derivatives of a series of anthra[1,9-*cd*:4,10-*c'd'*]bis[1,2]dithiole, diselenole, and ditellurole have been prepared as a new type of electron donor. The introduced methyl groups serve to enhance not only the donor strength, but also the solubility, enabling a ready formation of their charge-transfer complexes with various electron acceptors such as 7,7,8,8-tetracyanoquinodimethane (TCNQ), its 2,3,5,6-tetrafluoro derivative, 2,5-dimethyl derivative (DMTCNQ), 2,5-dimethoxy derivative (DMOTCNQ), 2,6-bis(dicyanomethylene)-2,6-dihydronaphthalene (TNAP), 3,3'-dichloro-5,5'-bis(dicyanomethylene)-$\Delta^{2,2'}$-bi(3-thiolene) (DCBT), and 3,3'-dibromo-5,5'-bis(dicyanomethylene)-$\Delta^{2,2'}$-bi(3-selenolene) (DBBS). Although the resulting complexes are mostly 1:1 stoichiometrical, the TCNQ complexes tend to favor a composition rich in acceptors; on the contrary, the DMTCNQ and DMOTCNQ complexes tend to favor a composition rich in donors. Their electrical conductivities range widely from 8 to 10^{-9} S cm^{-1}, being apparently dependent on appropriate combinations of the donors and the acceptors. In general, the present donors have a tendency to form highly conductive complexes with TCNQ, TNAP, DCBT, and DBBS. These highly conductive complexes mostly show a broad electron absorption in the infrared region, being characteristic of a segregated stacked structure in a mixed valence state. On the other hand, the X-ray analyses of DMTCNQ complexes of 3,4-dimethyl, 8,9-dimethyl, and 3,4,8,9-tetramethylanthra[1,9-*cd*:4,10-*c'd'*]diselenoles and 3,4,8,9-tetramethylanthra[1,9-*cd*:4,10-*c'd'*]dithiole have revealed that all of the crystal structures have mixed stack columns of donor–donor–acceptor type. Of them, the 3,4-dimethyl derivative complex shows an unusually high conductivity (0.53 S cm^{-1}) for a mixed stacked structure, which is considered to be due to strong heteroatomic interactions of the intra- and inter-columns.

Polyacenes bearing peri-dichalcogen bridges are known as prototypes of superior electron donors. A representative is naphthaceno[5,6-*cd*:11,12-*c'd'*]bis-[1,2]dithiole, abbreviated as tetrathiotetracene or TTT; it has a stronger donating ability than does tetrathiafulvalene (TTF).[1] However, it has a very low solubility in common solvents, limiting any wide study concerning its molecular complexes. Although the selenium isologue (TST)[1] and the tellurium isologue (TTeT)[2] have also aroused interest concerning the introduction of interactive heavy chalcogens, they are intractable because of their poorer solubilities. The lower polyacene homologues, anthra[1,9-*cd*:4,10-*c'd'*]bis[1,2]dithiole (tetrathioanthracene or TTA),[3] naphtho[1,8-*cd*:4,5-*c'd'*]bis-[1,2]dithiole (tetrathionaphthalene or TTN),[4] and their selenium isologues (TSA[5] and TSN[6]), have thus been studied as more tractable materials. However, their donor characters considerably decrease, and their solubilities are not so much improved as expected. In addition, their tellurium isologues still remain unknown. We previously investigated the 2,3,6,7-tetramethyl derivatives of tetrachalcogenonaphthalenes.[7] This structural modification allowed the formation of all of the chalcogen derivatives (TMTTN, TMTSN, and TMTTeN) involving the tellurium isologue. In addition, the introduced methyl groups served to enhance not only the donor strength, but also the solubility, enabling a detailed study of their complexes. We have further designed the same modification in other peri-dichalogenide polyacenes. We here report on the syntheses and properties of 2,3-dimethyl, 6,7-dimethyl, and 2,3,6,7-tetramethyl derivatives of tetrachalcogenoanthracenes and their charge-transfer complexes.[8]

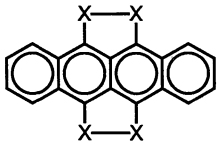

TTT, X=S
TST, X=Se
TTeT, X=Te

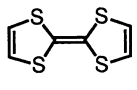

TTF

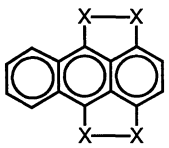

TTA, X=S
TSA, X=Se

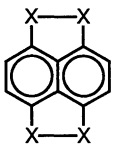

TTN, X=S
TSN, X=Se

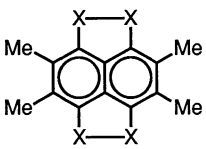

TMTTN, X=S
TMTSN, X=Se
TMTTeN, X=Te

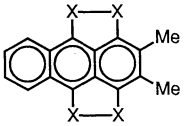

2,3-DMTTA, X=S
2,3-DMTSA, X=Se
2,3-DMTTeA, X=Te

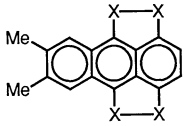

6,7-DMTTA, X=S
6,7-DMTSA, X=Se

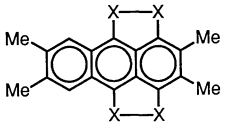

TMTTA, X=S
TMTSA, X=Se
TMTTeA, X=Te

Results and Discussion

Syntheses. Syntheses of dimethyl and tetramethyl tetrachalcogenoanthracenes were carried out according

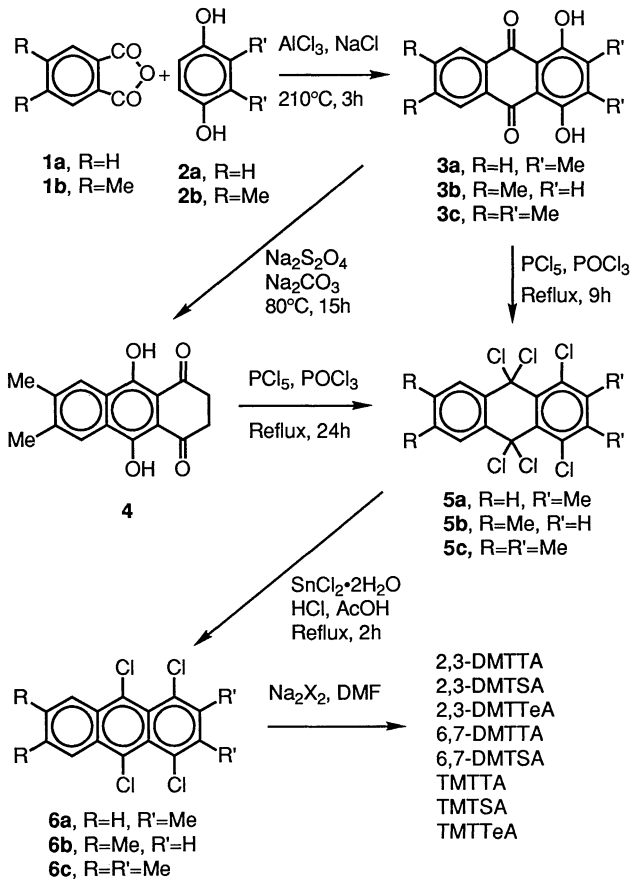

Scheme 1.

to Scheme 1. Thus 1,4-dihydroxy-2,3-dimethylanthraquinone (**3a**), prepared from a one-step condensation of phthalic anhydride (**1a**) with 2,3-dimethylhydroquinone (**2b**),[9] was allowed to react with phosphorus pentachloride to give 1,4,9,9,10,10-hexachloro-2,3-dimethyl-9,10-dihydroanthracene (**5a**) in 59% yield which, upon subsequent dechlorination with tin(II) chloride dihydrate, afforded 1,4,9,10-tetrachloro-2,3-dimethylanthracene (**6a**) in 75% yield. The treatment of **6a** with sodium disulfide, freshly prepared from sodium and sulfur, in refluxing *N*,*N*-dimethylformamide gave 2,3-dimethyltetrathioanthracene (2,3-DMTTA) in 43% yield. A similar reaction of **6a** with sodium diselenide gave the selenium isologue (2,3-DMTSA) in 31% yield. In contrast to an unsuccessful synthesis of the parent tetratelluroanthracene (TTeA), the tellurium isologue (2,3-DMTTeA) was obtained in 15% yield from a reaction of **6a** with sodium ditelluride at a lower temperature of 100 °C. The same approach to 6,7-dimethyl isomers from a combination of 4,5-dimethylphthalic anhydride (**1b**) and hydroquinone (**2a**) were unexpectedly troublesome regarding the following two steps. The first problem was that the treatment of 1,4-dihydroxy-6,7-dimethylanthraquinone (**3b**) with phosphorus pentachloride did not afford any amount of 1,4,9,9,10,10-hexachloro-6,7-dimethyl-9,10-dihydroanthracene (**5b**). Then, **3b** was reduced with sodium dithionite to 6,7-dimethylanthracene-1,4,9,10-tetrol, which mainly exists as the keto form, 2,3-dihydro-9,10-dihydroxy-6,7-dimethyl-1,4-anthracenedione (**4**) (88% yield). An alternative reaction of **4** with phosphorus pentachloride gave the desired hexachloro compound (**5b**) in 30% yield. The other problem arose in the last substitution reaction of the tetrachloro compound (**6b**) with sodium dichalcogenide. Although 6,7-dimethyltetraselenoanthracene (6,7-DMTSA) was obtained in 38% yield by the reaction, in spite of much effort 6,7-dimethyltetrathioanthracene (6,7-DMTTA) was obtained in only a trace yield and was hardly reproducible. Furthermore, no 6,7-dimethyltetratelluroanthracene was formed. On the other hand, a set of 2,3,6,7-tetramethyl derivatives (TMTTA, TMTSA, and TMTTeA) were smoothly completed by the same reaction sequence starting with a combination of **1b** and **2b**, as described for the 2,3-dimethyl derivatives.

Table 1. Half-Wave Oxidation Potentials of Peri-Dichalcogenide Donors[a)]

Compound	$E_{1/2}(1)$/V	$E_{1/2}(2)$/V	ΔE/V
TTA	0.36	0.75	0.39
TSA	0.35	0.71	0.36
2,3-DMTTA	0.32	0.73	0.41
2,3-DMTSA	0.31	0.72	0.41
2,3-DMTTeA	0.20	0.63	0.43
6,7-DMTTA	0.31	0.72	0.41
6,7-DMTSA	0.30	0.68	0.38
TMTTA	0.26	0.69	0.43
TMTSA	0.26	0.68	0.42
TMTTeA	0.16	0.55	0.39
TTT	0.19	0.56	0.37
TTF	0.34	0.72	0.38

a) Cyclic voltammetry was measured at 100 mV s^{-1} scan rate with Pt working and counter electrodes and Ag/AgCl reference electorde in 10^{-3} mol dm^{-3} benzonitrile solution containing 0.1 mol dm^{-3} tetrabutylammonium perchlorate as supporting electrolyte.

Oxidation Potentials. Cyclic voltammograms of all of the tetrachalcogenoanthracenes show two reversible one-electron redox waves; their half-wave oxidation potentials are summarized in Table 1. The first and second oxidation potentials of the parent TTA are almost comparable to the corresponding ones of TTF. The introduction of methyl groups actually lowers these values in the order of dimethylation and tetramethylation. The effect is more eminent in the first oxidation than in the second one. There is no essential difference between the enhanced effects due to dimethylation at the 2,3-positions and at the 6,7-positions. Substitution of selenium for sulfur in any series of the parent, dimethyl, and tetramethyl derivatives has little influence on the oxidation potentials. However, substitution of tellurium results in a considerable lowering of both the first and second potentials. As a result, 2,3-DMTTeA and TMTTeA have very strong donating abilities which are either comparable or superior to that of TTT.

Table 2. Charge-Transfer Complexes of Peri-Dichalcogenide Anthracenes

Complex	D:A	Appearance[a]	Dp	Found (Calcd)[b]/%			ν_{CN}	CT Band[c]	ΔE_{redox}[d]	σ[e]
			°C	C	H	N	cm^{-1}	$\times 10^3\ cm^{-1}$	V	$S\ cm^{-1}$
2,3-DMTTA·TCNQ	2:3	Black needles	214	64.66 (64.13	2.56 2.57	13.92 13.20)	2206	3.1, 10.1	0.13	9.6×10^{-1}
2,3-DMTSA·TCNQ	1:2	Black needles	238	52.56 (51.85	1.95 1.96	11.40 12.09)	2203	2.8, 9.9, 11.4	0.12	1.2
2,3-DMTTeA·TCNQ	1:1	Black needles	>300	36.58 (36.68	1.49 1.54	5.55 6.11)	2186	10.2	0.01	5.3×10^{-6}
6,7-DMTSA·TCNQ	1:1	Blue-black powder	245	47.49 (46.56	1.95 1.95	7.31 7.75)	2202	3.2, 11.5	0.11	2.0
TMTTA·TCNQ	1:2	Black needles	220	65.50 (65.78	3.10 2.89	13.81 14.61)	2204	3.3, 11.5, 13.0	0.07	5.0×10^{-2}
TMTSA·TCNQ	1:2	Black needles	237	53.32 (53.03	2.58 2.11	11.00 10.71)	2207	6.1, 10.0, 11.5	0.07	2.7×10^{-1}
TMTTeA·TCNQ	1:1	Black fine needles	>300	39.04 (38.13	2.11 1.92	5.33 5.93)	2187	10.0	−0.03	1.8×10^{-6}
2,3-DMTTA·TCNQF$_4$	1:1	Black powder	>300	55.78 (55.44	1.55 1.66	9.31 9.24)	2200	11.2	−0.28	2.2×10^{-6}
2,3-DMTSA·TCNQF$_4$	1:1	Purple powder	>300	42.05 (42.34	1.17 1.27	7.00 7.05)	2199	11.2	−0.29	5.4×10^{-6}
2,3-DMTTeA·TCNQF$_4$	1:1	Black powder	>300	34.80 (34.01	1.02 1.02	6.11 5.67)	2198	10.5	−0.40	1.8×10^{-7}
6,7-DMTSA·TCNQF$_4$	1:1	Black needles	>300	42.17 (42.34	1.33 1.27	6.06 7.05)	2200	11.0	−0.30	8.8×10^{-5}
TMTTA·TCNQF$_4$	1:1	Purple powder	240	56.53 (56.77	2.00 2.22	9.72 8.83)	2202	11.3	−0.34	5.0×10^{-7}
TMTSA·TCNQF$_4$	1:1	Purple powder	270	43.52 (43.82	1.62 1.72	6.82 6.81)	2201	11.1	−0.34	5.2×10^{-7}
TMTTeA·TCNQF$_4$	1:1	Dark blue powder	>300	35.43 (35.44	1.41 1.39	5.43 5.51)	2201	11.4	−0.44	4.4×10^{-6}
2,3-DMTTA·DMTCNQ	2:1	Black needles	219	62.37 (61.85	3.41 3.16	6.49 6.27)	2198	3.3, 11.2	0.20	9.5×10^{-1}
2,3-DMTSA·DMTCNQ	2:1	Black needles	236	44.25 (43.56	2.32 2.22	4.49 4.42)	2172	4.6, 11.3, 12.6	0.19	5.3×10^{-1}
2,3-DMTTeA·DMTCNQ	2:1	Black needles	>300	33.29 (33.13	2.29 1.70	3.85 3.58)	2186	10.2	0.08	1.2×10^{-3}
6,7-DMTSA·DMTCNQ	2:1	Black needles	262	44.09 (43.55	2.18 2.22	4.25 4.42)	2190	5.4, 11.6	0.18	2.7×10^{-8}
TMTTA·DMTCNQ	2:1	Black needles	241	63.72 (63.26	3.88 3.82	6.57 5.90)	2214	Non	0.14	7.4×10^{-7}
TMTSA·DMTCNQ	2:1	Black needles	>300	46.29 (45.34	2.94 2.74	4.25 4.23)	2210	11.5	0.14	1.2×10^{-5}
TMTTeA·DMTCNQ	2:1	Black powder	>300	35.56 (35.04	2.37 2.12	3.68 3.26)	2183	10.2	0.04	4.6×10^{-2}
2,3-DMTTA·DMOTCNQ	1:1	Black needles	266	46.17 (46.06	2.80 2.32	6.74 7.16)	2204	3.7, 10.3	0.31	2.2
2,3-DMTSA·DMOTCNQ	1:1	Black needles	269	60.91 (60.59	3.43 3.05	9.32 9.42)	2208	6.9	0.32	5.0×10^{-7}
2,3-DMTTeA·DMOTCNQ	1:1	Black needles	>300	37.18 (36.89	1.86 1.86	5.57 5.74)	2190	10.3	0.19	3.2×10^{-2}

Table 2. (Continued)

Complex	D:A	Appearance[a]	Dp	Found (Calcd)[b]/%			ν_{CN}	CT Band[c]	ΔE_{redox}[d]	σ[e]
			°C	C	H	N	cm^{-1}	$\times 10^3\ cm^{-1}$	V	$S\ cm^{-1}$
6,7-DMTSA·DMOTCNQ	2:1	Black needles	270	43.12 (42.49	2.03 2.17	4.33 4.31)	2222	Non	0.29	1.9×10^{-9}
TMTTA·DMOTCNQ	2:1	Brown needles	283	61.36 (61.20	4.08 3.70	6.52 5.71)	2220	Non	0.25	4.0×10^{-9}
TMTSA·DMOTCNQ	2:1	Black needles	295	45.18 (44.27	2.60 2.67	4.12 4.13)	2219	Non	0.25	1.0×10^{-8}
TMTTeA·DMOTCNQ	2:1	Black powder	>300	35.00 (34.40	2.10 2.07	3.13 3.21)	2183	Non	0.15	1.1×10^{-7}
2.3-DMTTA·TNAP	1:1	Black fine needles	232	66.05 (65.73	2.64 2.76	9.42 9.58)	2200	2.3, 8.8	0.11	7.9
2,3-DMTSA·TNAP	1:1	Black fine needles	250	49.93 (49.76	2.16 2.09	7.30 7.25)	2205	3.5, 8.9	0.10	2.6×10^{-2}
2,3-DMTTeA·TNAP	1:1	Black power	>300	40.40 (39.75	1.63 1.67	5.55 5.79)	2187	8.5, 10.2	−0.01	4.9×10^{-2}
TMTTA·TNAP	1:1	Black powder	231	66.88 (66.64	3.23 3.29	8.90 9.14)	2202	2.4, 8.8	0.05	1.7
TMTSA·TNAP	1:1	Purple plates	>300	50.02 (51.02	2.59 2.52	6.73 7.00)	2184	8.8, 10.0	0.05	9.2×10^{-3}
TMTTeA·TNAP	1:1	Black powder	>300	41.59 (41.04	2.03 2.03	5.70 5.63)	2190	8.8, 10.3	−0.05	6.0×10^{-1}
2,3-DMTTA·DCBT	1:1	Dark green fine needles	>300	51.17 (52.09	2.02 1.75	7.86 8.10)	2216	5.9	0.16	1.5×10^{-6}
2,3-DMTSA·DCBT	1:1	Dark green fine needles	>300	40.94 (40.98	1.41 1.38	6.32 6.37)	2206	3.6	0.15	3.7
2,3-DMTTeA·DCBT	1:1	Dark green fine needles	>300	33.51 (33.55	1.21 1.13	5.03 5.22)	2196	3.5, 10.1	0.04	6.0
TMTTA·DCBT	1:1	Green fine needles	254	54.09 (53.40	2.16 2.24	6.78 7.78)	2201	5.1, 8.7	0.10	6.0×10^{-3}
TMTSA·DCBT	1:1	Green needles	280	42.18 (42.36	1.91 1.78	5.94 6.17)	2208	5.5, 8.7	0.10	3.1×10^{-3}
TMTTeA·DCBT	1:1	Black powder	>300	34.46 (34.88	1.51 1.46	4.80 5.08)	2199	3.5, 8.5, 10.1	0	2.3
2,3-DMTTA·DBBS	1:1	Dark green fine needles	>300	42.16 (41.21	1.62 1.38	6.20 6.41)	2216	3.5, 8.3	0.20	7.1×10^{-1}
2,3-DMTSA·DBBS	1:1	Dark green plates	>300	33.95 (33.93	1.29 1.14	5.23 5.27)	2198	3.4, 8.3	0.19	8.0
2,3-DMTTeA·DBBS	1:1	Dark green powder	>300	28.81 (28.68	1.19 0.96	4.40 4.46)	2200	3.4, 10.0	0.08	5.8
TMTTA·DBBS	1:1	Dark green needles	>300	42.94 (42.59	2.17 1.79	5.48 6.21)	2212	5.0, 8.7	0.14	1.0×10^{-3}
TMTSA·DBBS	1:1	Dark green needles	>300	35.71 (35.26	1.45 1.48	4.38 5.14)	2208	5.5, 8.7	0.14	8.1×10^{-4}
TMTTeA·DBBS	1:1	Black powder	>300	30.08 (29.92	1.25 1.26	4.34 4.36)	2202	3.3, 9.9	0.04	3.6

a) Obtained from chlorobenzene. b) Calculated as stoichiometry indicated for the complex. c) Measured with a KBr disk method. d) $\Delta E_{redox}=E_{1/2}(D)-E_{1/2}(A)$.
e) Measured on compressed pellets at RT with a two-probe or four-probe method.

Molecular Complexes. The methyl group of the present tetrachalcogenoanthracenes actually contributes to enhance their solubilities. This effect, however, is more remarkable in dimethylation than in tetramethylation. For example, the molar solubilities of a series of tetraselenoanthracenes in chloroform are as follows: TSA 2.1×10^{-4} mol dm^{-3}, 2,3-DMTSA 3.1×10^{-3} mol dm^{-3}, 6,7-DMTSA 8.5×10^{-4} mol dm^{-3}, and TMTSA 3.2×10^{-4} mol dm^{-3}. The stronger donating abilities and better solubilities of the dimethyl and tetramethyl derivatives than parent tetrachalcogenoanthracenes facilitated a study of their complexation. They thus gave a number of charge-transfer complexes, as summarized in Table 2. The acceptors used in this experiment involve not only those of well-known classes such as 7,7,8,8-tetracyanoquinodimethane (TCNQ), its 2,3,5,6-tetrafluoro derivative ($TCNQF_4$), 2,5-dimethyl derivative (DMTCNQ), 2,5-dimethoxy derivative (DMOTCNQ), and 2,6-bis(dicyanomethylene)-2,6-dihydronaphthalene (a common name: 9,9,10,10-tetracyano-2,6-naphthoquinodimethane or TNAP) but also of new types such as 3,3'-dichloro-5,5'-bis(dicyanomethylene)-$\Delta^{2,2'}$-bi(3-thiolene) (DCBT)[10] and 3,3'-dibromo-5,5'-bis(dicyanomethylene)-$\Delta^{2,2'}$-bi(3-selenolene) (DBBS).[11] The half-

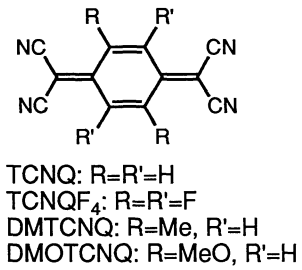

TCNQ: R=R'=H
$TCNQF_4$: R=R'=F
DMTCNQ: R=Me, R'=H
DMOTCNQ: R=MeO, R'=H

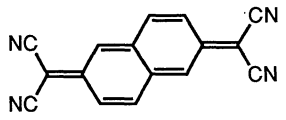

TNAP

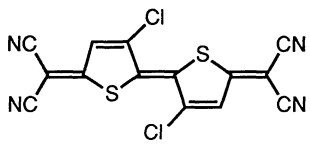

DCBT

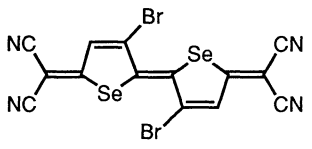

DBBS

wave reduction potentials and infrared nitrile frequencies of these acceptors are given in Table 3. The reduction potentials, except for that of $TCNQF_4$, are just appropriate to form conductive complexes with the present donors; the differences ΔE_{redox} between the oxidation potentials of the donors and the reduction potentials of the acceptors are in the range from −0.05 V to 0.32 V, which has a high probability of being organic metals.[12] The resulting complexes are mostly 1 : 1 stoichiometrical, but some complexes favor a composition rich in either donors or acceptors, even when both components are mixed in equimolar amounts. In addition, their electrical conductivities widely range from 8 to 10^{-9} S cm^{-1}, being independent of the stoichiometry. The stoichiometry and conductivities are apparently dependent on appropriate combinations of the donors and acceptors, but can be somewhat systematized according to the used acceptors rather than the donors, as follows. The TCNQ complexes of the TTA and TSA derivatives tend to favor a composition rich in acceptor species, and the electrical conductivities measured on compressed pellets at room temperature are in the high range of 0.05—2.0 S cm^{-1}. These complexes, except for the TMTSA complex, show a broad electron absorption in the infrared region, being characteristic of a segregated stacked structure in a mixed valence state.[13] The incomplete charge transfer was also supported by nitrile vibrational frequencies, which are intermediate between those of neutral TCNQ (2232 cm^{-1}) and Na^+TCNQ^- (2174 cm^{-1}).[14] In contrast, the TCNQ complexes of stronger tellurium-containing donors, DMTTeA and TMTTeA, have the 1 : 1 composition and low conductivities. All of the complexes with a stronger acceptor, $TCNQF_4$, are also 1 : 1 stoichiometrical and exhibit a low conductivity. These low conductivity complexes must correspond to Mott insulators, since the increasing donor or acceptor character causes a complete charge transfer, as indicated by the low frequencies of the infrared nitrile vibrations. On the other hand, a weaker acceptor DMTCNQ takes complexes of a 2 : 1 composition rich in donor, reflecting increasing bulkiness of the acceptors. These complexes mostly exhibit a low conductivity, and the electronic spectra indicate segregated stacking only for a complex with 2,3-DMTTA. A similar result was observed for the DMOTCNQ complexes. Some of the DMTCNQ complexes were actually confirmed by X-ray crystallographic analyses to take mixed stacking, which is further discussed later in connection with their conductivities. The other acceptors (TNAP, DCBT, and DBBS) are strong electron acceptors comparable to TCNQ and have additional advantages of high polarization and reduced Coulomb repulsion due to their extensive conjugation. Their complexes are all 1 : 1 stoichiometrical and mostly high-conductive, indicating mutual fitness of the donors and the acceptors. The enhanced intermolecular interactions of the individual components due to the

Table 3. Half-Wave Reduction Potentials[a] and Nitrile Vibrational Frequencies of Electron Acceptors

Compound	$E_{1/2}(1)$/V	$E_{1/2}(2)$/V	ΔE/V	ν_{CN}/cm^{-1}
TCNQ	0.19	−0.43	0.62	2232
$TCNQF_4$	0.60	−0.05	0.65	2234
DMTCNQ	0.12	−0.42	0.54	2230
DMOTCNQ	0.01	−0.52	0.53	2225
TNAP	0.21	−0.21	0.42	2225
DCBT	0.16	−0.09	0.25	2217
DBBS	0.12	−0.10	0.22	2220

a) Cyclic voltammetry was measured at 100 mV s^{-1} scan rate with Pt working and counter electrodes and Ag/AgCl reference electorde in 10^{-3} mol dm^{-3} benzonitrile solution containing 0.1 mol dm^{-3} tetrabutylammonium perchlorate as supporting electrolyte.

Table 4. Crystal Data of DMTCNQ Complexes

	2,3-DMTSA	6,7-DMTSA	TMTSA	TMTTA
Formula	$C_{46}H_{28}N_4Se_8$	$C_{46}H_{28}N_4Se_8$	$C_{50}H_{36}N_4Se_8$	$C_{50}H_{36}N_4S_8$
Fw	1268.44	1268.44	1324.54	949.37
Crystal system	Monoclinic	Monoclinic	Monoclinic	Monoclinic
Space group	$P2_1/n$	$P2_1/n$	$P2_1/n$	$P2_1/n$
a/Å	8.869(1)	16.561(4)	10.027(1)	9.942(1)
b/Å	20.322(2)	11.532(3)	20.852(2)	20.542(2)
c/Å	11.132(2)	10.901(3)	10.613(1)	10.500(1)
β/°	91.14(1)	99.22(2)	99.06(1)	98.65(1)
V/Å^3	2005.9(4)	2054.9(9)	2191.4(4)	2120.1(4)
Z	2	2	2	2
Crystal size/mm^3	0.24×0.04×0.01	0.33×0.13×0.08	0.41×0.06×0.01	0.50×0.10×0.08
Abs correction	Analytical[a)]	None	None	Analytical[a)]
No. of data	2423	2538	2333	2623
R	0.045	0.068	0.070	0.069

a) Ref. 18.

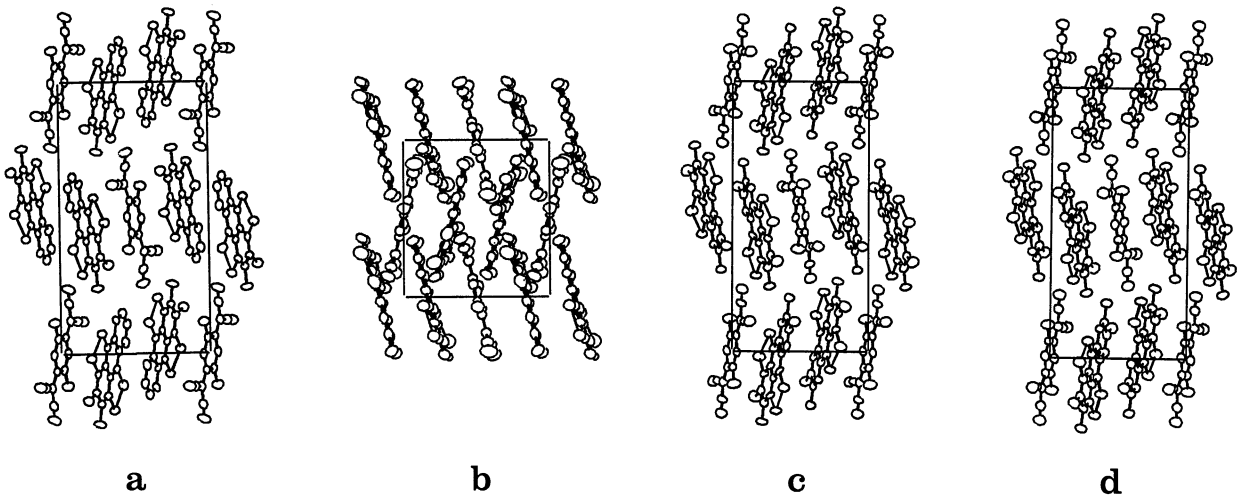

Fig. 1. Crystal structures of DMTCNQ complexes with 2,3-DMTSA (a), 6,7-DMTSA (b), TMTSA (c), and TMTTA (d) projected along the a axis.

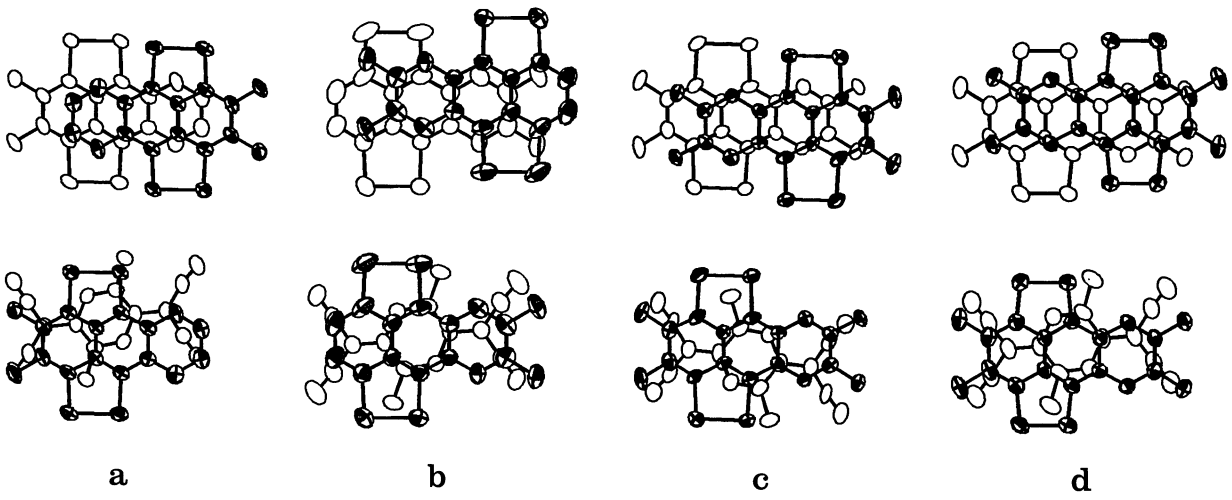

Fig. 2. Molecular overlapping modes of DMTCNQ complexes with 2,3-DMTSA (a), 6,7-DMTSA (b), TMTSA (c), and TMTTA (d) viewed perpendicular to the molecular planes.

Table 5. Intramolecular Bond Distances and Angles for DMTCNQ Complexes

Bond distance/Å	2,3-DMTSA	6,7-DMTSA	TMTSA	TMTTA
X1–X2	2.319(1)	2.342(1)	2.331(2)	2.091(2)
X1–C16	1.885(7)	1.909(8)	1.904(11)	1.746(5)
X2–C3	1.894(7)	1.901(10)	1.930(11)	1.762(6)
C3–C4	1.379(10)	1.350(13)	1.344(16)	1.378(8)
C3–C17	1.426(10)	1.440(13)	1.462(16)	1.424(8)
C4–C5	1.398(11)	1.448(18)	1.430(17)	1.441(9)
C4–C19	1.520(11)	—	1.525(18)	1.512(9)
C5–C6	1.369(11)	1.383(17)	1.391(17)	1.372(8)
C5–C20	1.533(10)	—	1.506(17)	1.528(9)
C6–X7	1.904(8)	1.890(12)	1.926(12)	1.762(6)
C6–C18	1.437(10)	1.427(14)	1.387(15)	1.423(7)
X7–X8	2.328(1)	2.353(2)	2.335(2)	2.090(2)
X8–C9	1.896(7)	1.899(9)	1.923(12)	1.760(6)
C9–C10	1.421(10)	1.402(13)	1.384(15)	1.403(8)
C9–C18	1.377(10)	1.384(14)	1.431(16)	1.386(7)
C10–C11	1.436(11)	1.419(14)	1.412(15)	1.409(7)
C10–C15	1.436(10)	1.442(12)	1.447(15)	1.456(7)
C11–C12	1.379(11)	1.383(15)	1.347(17)	1.376(8)
C12–C13	1.401(12)	1.418(16)	1.436(16)	1.448(8)
C12–C21	—	1.544(16)	1.542(16)	1.504(8)
C13–C14	1.370(12)	1.388(14)	1.381(16)	1.368(8)
C13–C22	—	1.505(15)	1.502(16)	1.504(8)
C14–C15	1.461(10)	1.403(12)	1.424(16)	1.428(7)
C15–C16	1.413(10)	1.412(12)	1.422(15)	1.409(7)
C16–C17	1.382(9)	1.377(12)	1.374(15)	1.391(7)
C17–C18	1.422(10)	1.451(13)	1.418(15)	1.412(7)
C23–C24	1.417(11)	1.445(12)	1.491(18)	1.447(9)
C23–C25′	1.405(10)	1.462(12)	1.430(17)	1.435(8)
C23–C26	1.438(10)	1.347(12)	1.388(17)	1.383(8)
C24–C25	1.369(11)	1.357(12)	1.340(17)	1.340(8)
C24–C31	1.547(11)	1.540(12)	1.529(18)	1.521(10)
C26–C27	1.445(11)	1.443(15)	1.417(18)	1.428(9)
C26–C29	1.395(12)	1.462(13)	1.416(20)	1.454(11)
C27–N28	1.120(11)	1.155(17)	1.125(17)	1.132(10)
C29–N30	1.145(13)	1.130(14)	1.126(20)	1.155(11)
Bond angle/°	**2,3-DMTSA**	**6,7-DMTSA**	**TMTSA**	**TMTTA**
X2–X1–C16	92.0(2)	91.1(3)	91.8(3)	95.9(2)
X2–X1–C3	92.0(2)	92.7(3)	93.2(3)	95.8(2)
X2–C3–C4	121.7(6)	122.4(8)	122.2(9)	124.5(4)
X2–C3–C17	116.2(5)	115.5(7)	113.2(7)	112.9(4)
C4–C3–C17	122.1(7)	122.1(9)	124.5(11)	122.6(5)
C3–C4–C5	119.6(7)	120.2(10)	120.5(11)	118.3(5)
C3–C4–C19	119.8(7)	—	118.4(11)	120.3(6)
C5–C4–C19	120.5(6)	—	121.2(11)	121.5(6)
C4–C5–C6	119.7(6)	119.2(10)	116.0(11)	119.8(5)
C4–C5–C20	121.2(7)	—	123.0(11)	120.3(6)
C6–C5–C20	119.1(7)	—	120.9(11)	119.9(6)
C5–C6–X7	121.5(5)	122.0(9)	119.3(8)	125.2(4)
C5–C6–C18	122.9(7)	122.2(11)	124.6(11)	122.0(5)
X7–C6–C18	115.6(5)	115.6(8)	116.1(9)	112.8(4)
C6–X7–X8	92.1(2)	91.8(4)	92.3(3)	95.9(2)
X7–X8–C9	92.2(2)	91.1(3)	92.3(3)	95.9(2)
X8–C9–C10	121.0(5)	120.8(7)	120.8(9)	124.3(4)
X8–C9–C18	117.3(5)	116.7(7)	115.3(8)	113.8(4)
C10–C9–C18	121.8(6)	122.4(8)	123.9(10)	121.9(5)
C9–C10–C11	122.5(7)	122.8(8)	123.5(10)	123.1(5)
C9–C10–C15	117.7(6)	118.8(8)	118.4(10)	118.2(5)
C11–C10–C15	119.8(7)	118.5(8)	118.2(10)	118.7(5)
C10–C11–C12	119.7(7)	121.1(9)	122.1(11)	122.5(5)
C11–C12–C13	121.0(8)	120.5(10)	120.9(11)	119.3(5)
C11–C12–C21	—	118.5(10)	121.3(10)	119.8(5)
C13–C12–C21	—	121.0(9)	117.8(11)	120.9(5)

Table 5. (Continued)

Bond angle/°	2,3-DMTSA	6,7-DMTSA	TMTSA	TMTTA
C12–C13–C14	121.9(7)	119.0(9)	119.0(10)	119.3(5)
C12–C13–C22	—	121.3(10)	121.9(10)	119.8(5)
C14–C13–C22	—	119.7(10)	119.0(10)	120.9(5)
C13–C14–C15	119.6(7)	122.2(9)	121.1(10)	122.7(5)
C10–C15–C14	118.0(7)	118.8(8)	118.7(10)	117.5(5)
C10–C15–C16	119.6(6)	118.4(8)	117.9(10)	119.1(5)
C14–C15–C16	122.4(7)	122.8(8)	123.4(10)	123.4(5)
X1–C16–C15	121.1(5)	119.8(6)	120.5(8)	125.0(4)
X1–C16–C17	117.7(5)	118.0(7)	117.6(8)	114.3(4)
C15–C16–C17	121.2(7)	122.2(8)	122.0(10)	120.7(5)
C3–C17–C16	121.9(6)	122.5(8)	123.9(10)	121.0(5)
C3–C17–C18	118.7(6)	118.3(8)	114.4(9)	118.6(5)
C16–C17–C18	119.4(6)	119.2(8)	121.7(10)	120.5(5)
C6–C18–C9	122.8(7)	123.2(9)	124.0(10)	121.6(5)
C6–C18–C17	117.0(6)	118.0(9)	120.0(10)	118.8(5)
C9–C18–C17	120.2(6)	118.9(8)	116.0(10)	119.7(5)
C24–C23–C25′	118.1(6)	117.7(7)	117.1(10)	117.5(5)
C24–C23–C26	123.8(7)	124.8(8)	123.3(11)	122.9(5)
C25′–C23–C26	118.2(7)	117.5(8)	119.6(11)	119.7(6)
C23–C24–C25	118.1(7)	119.3(8)	118.8(11)	119.4(5)
C23–C24–C31	124.9(7)	121.7(8)	122.7(11)	126.6(5)
C25–C24–C31	117.1(7)	118.8(8)	118.5(11)	114.1(6)
C23–C25–C24	123.9(7)	122.9(7)	124.1(11)	123.2(5)
C23–C26–C27	126.1(7)	129.0(9)	127.3(12)	126.8(6)
C23–C26–C29	118.9(7)	121.5(9)	119.7(11)	121.9(6)
C27–C26–C29	115.0(7)	109.5(8)	113.0(11)	111.3(6)
C26–C27–N28	172.6(9)	173.8(11)	172.7(16)	174.7(7)
C26–C29–N30	177.4(11)	179.0(13)	175.1(15)	176.6(7)

extended π-systems as well as interactive heteroactoms are considered to lead to a ready formation of segregated columns. In particular, it is worth noting that the tellurium-containing donors can form highly conductive complexes with these acceptors.

Crystal Structures of DMTCNQ Complexes. The four DMTCNQ complexes with 2,3-DMTSA, 6,7-DMTSA, TMTSA, and TMTTA offered good single crystals for X-ray analysis. Table 4 shows their crystal data, in which all crystals belong to the monoclinic space group. Of these complexes, only the 2,3-DMTSA complex has a high conductivity (0.53 S cm^{-1}) and an electronic absorption band at 4.6×10^3 cm^{-1}. Although it is expected to have a different crystal structure, all of the DMTCNQ complexes are isostructural with mixed stacked columns of a donor–donor–acceptor sequence along the *c*-axis (Fig. 1). In addition, overlapping modes for donor–donor and donor–acceptor are quite similar (Fig. 2). Their infrared nitrile vibrations as compared with that (2230 cm^{-1}) of neutral DMTCNQ indicate a complete charge-transfer for the 2,3-DMTSA complex (2172 cm^{-1}) but some charge-transfer for the 6,7-DMTSA complex (2190 cm^{-1}), the TMTTA complex (2214 cm^{-1}), and the TMTSA complex (2210 cm^{-1}). The actual charge-transfer of the 2,3-DMTSA complex is also supported by a detailed consideration of the molecular structures of the components (Fig. 3, Table 5).

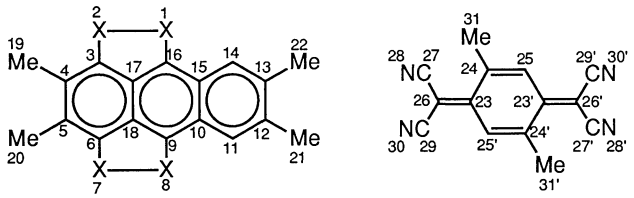

Fig. 3. Atomic numbering scheme for X-ray crystal structure analysis.

Because the strong donating character of the peri-dichalcogenide polyacenes is based on aromatization of the heterocyclic ring in the resulting cationic species, a charge-transfer in their complexes might bring about a change in the ring dimensions: that is, a shortening of the Se–Se and Se–C bond lengths.[15] For a comparison the molecular structures of neutral 2,3-DMTSA, 6,7-DMTSA, and 2,3-DMTTA were determined. 2,3-DMTSA was analyzed for a single crystal including one benzene per two molecules. The crystal data and the molecular structures are given in Tables 6 and 7, respectively. Since TMTTA and TMTSA did not offer good crystals for X-ray analyses, neutral 2,3-DMTTA and 2,3-DMTSA were used as substitutes for examining any dimensional change. Both the Se–Se and C–Se bond lengths of the 2,3-DMTSA complex are shorter

Table 6. Crystal Data of 2,3-DMTSA, 6,7-DMTSA, and 2,3-DMTTA

	$(2,3\text{-DMTSA})_2C_6H_6$	6,7-DMTSA	2,3-DMTTA
Formula	$C_{38}H_{26}Se_8$	$C_{16}H_{10}Se_4$	$C_{16}H_{10}S_4$
Fw	1114.30	518.10	330.51
Crystal system	Monoclinic	Monoclinic	Triclinic
Space group	$P2_1/n$	$P2_1/c$	$P\bar{1}$
a/Å	18.354(1)	7.509(1)	10.343(2)
b/Å	16.199(2)	22.028(2)	12.496(2)
c/Å	5.679(1)	9.471(1)	7.456(2)
α/°	90.0	90.0	90.15(2)
β/°	93.51(1)	111.41(1)	108.14(2)
γ/°	90.0	90.0	129.37(1)
V/Å^3	1685.3(4)	1458.4(3)	681.2(3)
Z	2	4	2
Crystal size/mm^3	0.64×0.08×0.06	0.35×0.10×0.02	0.35×0.13×0.10
Abs correction	Analytical[a)]	Analytical[a)]	Analytical[a)]
No. of data	2274	1874	1853
R	0.041	0.041	0.059

a) Ref. 18.

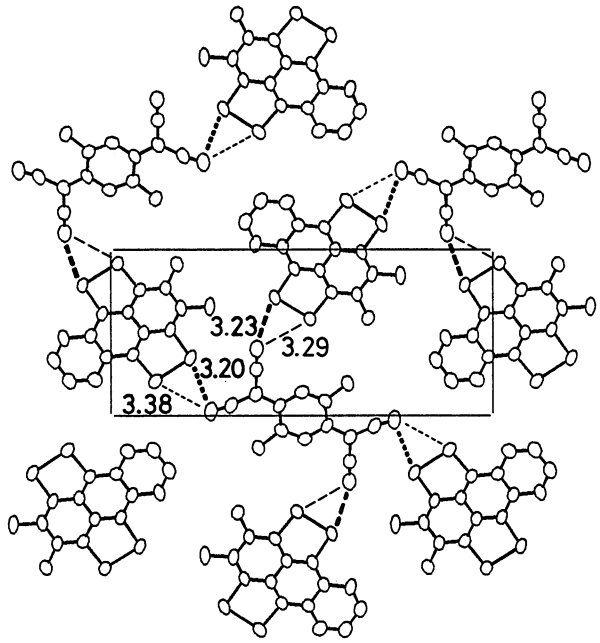

Fig. 4. Crystal structure of 2,3-DMTSA·DMTCNQ projected along the c axis.

than the corresponding ones of neutral 2,3-DMTSA, while the other complexes do not show such appreciable variations. In addition, the molecular geometry of DMTCNQ becomes more benzenoid in character for the 2,3-DMTSA·DMTCNQ complex (Table 5), supporting a complete charge transfer.[16] A question is why only the 2,3-DMTSA·DMTCNQ complex shows so large charge-transfer and high conductivity. As already pointed out, although its crystal structure is very similar to those of the other complexes, there is a small difference in overlapping distances. Thus the 2,3-DMTSA·DMTCNQ complex has a rather longer interplanar distance between the donor and acceptor than do the other omplexes, being in conflict with the actual degree of charge transfer. On the other hand, the interplanar distance between paired donors is shorter, and a short Se–Se contact (3.62 Å) is observed. In addition, there are observed some intercolumnar Se–N contacts between 2,3-DMTSA and the neighboring DMTCNQ, constituting a net-work sheet (Fig. 4). It is thus concluded that the large charge transfer and high conductivity of the 2,3-DMTSA·DMTCNQ complex are induced by strong heteroatomic interactions of Se–Se and Se–N.

Experimental

General. Melting points are uncorrected. All chemicals and solvent are of reagent grade. Elemental analyses were measured by Mr. Hideaki Iwatani, Microanalytical Laboratory in Department of Applied Chemistry, Faculty of Engineering, Hiroshima University. NMR spectra were recorded on a JEOL PMX-60 spectrometer (60 MHz) using deuteriochloroform as a solvent and tetramethylsilane as an internal standard. IR spectra were taken on a Hitachi 260-30 spectrometer with a KBr disk method. MS spectra were measured at 70 eV on a Shimadzu QP-1000A spectrometer using a direct insertion technique. Electronic spectra were recorded on a Shimadzu UV-160 spectrometer or on a Hitachi 330 spectrophotometer. Cyclic voltammetry was carried out on a Hokuto Denko HA-301 potentiostat and a Hokuto Denko HB-104 function generator.

1,4-Dihydroxy-2,3-dimethylanthraquinone (3a). Compound (**3**) was prepared by modifying the synthetic method of Kerdersky et al.[9] A mixture of anhydrous aluminium chloride (50 g) and sodium chloride (10 g) was well ground together in a mortor, and heated at 210 °C to melt. Into a stirred solution was added a mixture of phthalic anhydride (**1a**) (7.4 g, 50 mmol) and 2,3-dimethylhydroquinone (**2b**) (6.9 g, 50 mmol); heating at the temperature was continued for further 4 h. Concd hydrochloric acid (50 cm^3) and water (200 cm^3) were successively added into a mixture cooled to ca. 100 °C, which was then gently boiled for 2 h. The resulting solid, while still hot, was collected by filtration and dissolved in chloroform (2 dm^3). After the solution was filtered, the filtrate was concen-

Table 7. Intramolecular Bond Distances and Angles for 2,3-DMTSA, 6,7-DMTSA, and 2,3-DMTTA

Bond distance/Å	2,3-DMTSA	6,7-DMTSA	2,3-DMTTA
X1–X2	2.336(1)	2.344(1)	2.102(3)
X1–C16	1.912(6)	1.906(6)	1.760(4)
X2–C3	1.913(6)	1.913(6)	1.755(5)
C3–C4	1.382(8)	1.352(9)	1.388(10)
C3–C17	1.421(8)	1.429(9)	1.400(7)
C4–C5	1.417(8)	1.440(9)	1.442(7)
C4–C19	1.521(9)	—	1.520(8)
C5–C6	1.380(8)	1.364(10)	1.378(8)
C5–C20	1.508(8)	—	1.520(12)
C6–X7	1.915(6)	1.899(6)	1.763(4)
C6–C18	1.440(8)	1.441(9)	1.409(10)
X7–X8	2.345(1)	2.339(1)	2.090(3)
X8–C9	1.922(5)	1.898(6)	1.748(5)
C9–C10	1.405(8)	1.424(9)	1.421(10)
C9–C18	1.369(8)	1.372(10)	1.390(7)
C10–C11	1.433(9)	1.414(10)	1.420(8)
C10–C15	1.440(8)	1.430(8)	1.433(7)
C11–C12	1.393(9)	1.373(9)	1.388(13)
C12–C13	1.411(10)	1.422(10)	1.401(9)
C12–C21	—	1.527(11)	—
C13–C14	1.382(9)	1.399(10)	1.379(10)
C13–C22	—	1.513(10)	—
C14–C15	1.426(8)	1.415(9)	1.420(12)
C15–C16	1.414(8)	1.413(9)	1.405(8)
C16–C17	1.381(8)	1.393(8)	1.393(10)
C17–C18	1.443(8)	1.436(8)	1.419(6)
Bond angle/°	**2,3-DMTSA**	**6,7-DMTSA**	**2,3-DMTTA**
X2–X1–C16	91.6(2)	91.8(2)	95.7(3)
X1–X2–C3	92.3(2)	92.1(2)	95.3(2)
X2–C3–C4	120.9(4)	121.3(5)	124.2(4)
X2–C3–C17	115.7(4)	115.4(4)	114.1(5)
C4–C3–C17	123.4(5)	123.3(6)	121.7(4)
C3–C4–C5	119.6(5)	119.3(7)	119.0(5)
C3–C4–C19	120.2(5)	—	120.6(5)
C5–C4–C19	120.2(5)	—	120.4(6)
C4–C5–C6	118.3(5)	119.5(6)	118.8(7)
C4–C5–C20	121.4(5)	—	120.7(5)
C6–C5–C20	120.2(5)	—	120.6(5)
C5–C6–X7	121.0(4)	121.7(5)	124.2(5)
C5–C6–C18	124.1(5)	122.3(6)	122.6(4)
X7–C6–C18	114.9(4)	116.0(5)	113.3(4)
C6–X7–X8	92.4(2)	92.1(2)	95.4(2)
X7–X8–C9	91.5(2)	91.7(2)	96.0(2)
X8–C9–C10	120.5(4)	120.3(5)	125.1(3)
X8–C9–C18	116.9(4)	117.9(5)	113.9(5)
C10–C9–C18	122.6(5)	121.7(5)	121.0(4)
C9–C10–C11	122.6(5)	122.9(6)	121.8(5)
C9–C10–C15	118.5(5)	118.7(6)	118.7(5)
C11–C10–C15	118.9(5)	118.3(5)	119.5(7)
C10–C11–C12	119.8(6)	121.9(6)	119.8(5)
C11–C12–C13	120.7(6)	120.4(7)	120.8(6)
C11–C12–C21	—	119.8(6)	—
C13–C12–C21	—	119.7(6)	—
C12–C13–C14	121.2(6)	118.8(6)	120.6(9)
C12–C13–C22	—	120.5(6)	—
C14–C13–C22	—	119.7(6)	—
C13–C14–C15	119.8(6)	121.3(6)	120.6(6)
C10–C15–C14	119.6(5)	119.2(6)	118.8(5)
C10–C15–C16	118.3(5)	118.8(5)	118.9(6)
C14–C15–C16	122.1(5)	121.9(6)	122.3(5)
X1–C16–C15	120.5(4)	121.3(4)	124.3(6)
X1–C16–C17	117.2(4)	116.8(5)	113.6(4)
C15–C16–C17	122.3(5)	121.8(5)	122.0(4)
C3–C17–C16	123.2(5)	123.3(5)	121.4(4)
C3–C17–C18	117.9(5)	117.7(5)	120.0(6)
C16–C17–C18	118.9(5)	119.0(6)	118.9(5)
C6–C18–C9	123.9(5)	122.3(5)	121.4(4)
C6–C18–C17	116.6(5)	117.8(6)	118.3(5)
C9–C18–C17	119.4(5)	119.9(6)	120.4(6)

trated to ca. 200 cm³ and purified by column chromatography on silica gel using chloroform as an eluent to give a reddish-orange solid of **3a** (11.3 g, 84.6%). An analytical sample was obtained as reddish-orange needles upon recrystallization from benzene–hexane: Mp 259—260 °C (lit,[9] mp 252—253 °C); ^{1}H NMR δ=2.40 (s, 6H, CH_3), 7.73 (AA'BB' m, 2H, ArH), 8.24 (AA'BB' m, 2H, ArH), and 13.48 (s, 2H, OH); IR 1590 cm^{-1} (C=O); MS *m/z* 268 (M^+); Anal. Calcd for $C_{16}H_{12}O_4$: C, 71.64; H, 4.51%. Found: C, 71.63; H, 4.51%.

1,4-Dihydroxy-6,7-dimethylanthraquinone (3b): 74% yield; reddish orange needles from chloroform; mp 228 °C; ^{1}H NMR δ=2.30 (s, 6H, CH_3), 7.20 (s, 2H, ArH), 7.95 (s, 2H, ArH), and 12.75 (s, 2H, OH); IR 1630 and 1590 cm^{-1} (C=O); MS *m/z* 268 (M^+); Anal. Calcd for $C_{16}H_{12}O_4$: C, 71.64; H, 4.51%. Found: C, 71.60; H, 4.49%.

1,4-Dihydroxy-2,3,6,7-tetramethylanthraquinone (3c): 69% yield; reddish orange needles from chloroform; mp 276 °C; ^{1}H NMR δ=2.25 (s, 6H, CH_3), 2.40 (s, 6H, CH_3), 7.96 (s, 2H, ArH), and 13.40 (s, 2H, OH); IR 1580 cm^{-1} (C=O); MS *m/z* 296 (M^+); Anal. Calcd for $C_{18}H_{16}O_4$: C, 72.96; H, 5.44%. Found: C, 72.84; H, 5.40%.

2,3-Dihydro-9,10-dihydroxy-6,7-dimethyl-1,4-anthracenedione (4). Into a suspension of **3b** (5.3 g, 19.8 mmol) and anhyd. sodium carbonate (5 g) in water (100 cm³) was added sodium dithionite (10 g); the mixture was heated at 80 °C for 15 h. After cooling, the resulting yellow solid was collected by filtration and dried. Chromatography on silica gel using dichloromethane as an eluent followed by recrystallization from benzene-hexane gave yellow needles of **4** (4.8 g, 88%): Mp 182 °C; ^{1}H NMR δ=2.45 (s, 6H, CH_3), 2.96 (s, 4H, CH_2), 8.00 (s, 2H, ArH), and 13.60 (s, 2H, OH); IR 1610 cm^{-1} (C=O); MS *m/z* 270 (M^+); Anal. Calcd for $C_{16}H_{14}O_4$: C, 71.11; H, 5.22%. Found: C, 71.40; H, 5.05%.

1,4,9,9,10,10-Hexachloro-2,3-dimethyl-9,10-dihydroanthracene (5a). A mixture of **3a** (4.2 g, 15.7 mmol), phosphorus pentachloride (23 g, 110 mmol), and phosphoryl oxychloride (40 cm³) was refluxed for 9 h. Concentration in a reduced pressure followed by thorough washing of the residue with hexane and then with methanol left a white solid of **5a** (3.8 g, 59%); mp 140 °C (decomp); ^{1}H NMR δ=2.55 (s, 6H, CH_3), 7.42 (AA'BB' m, 2H, ArH), and 7.95 (AA'BB' m, ArH); IR 710 cm^{-1} (C–Cl); MS *m/z* 414 (M^+) with an isotopic pattern hexachlorine. Anal. Calcd for $C_{16}H_{10}Cl_6$: C, 46.31; H, 2.43%. Found: C, 45.71; H, 2.36%.

1,4,9,9,10,10-Hexachloro-6,7-dimethyl-9,10-dihydroanthracene (5b): 30% yield from **4**; a white solid; mp 232 °C (decomp); ^{1}H NMR δ=2.45 (s, 6H, CH_3), 7.52 (s, 2H, ArH), and 7.73 (s, 2H, ArH); IR 740 cm^{-1} (C–Cl); MS *m/z* 414 (M^+) with an isotopic pattern of hexachlorine. Anal. Calcd for $C_{16}H_{10}Cl_6$: C, 46.31; H, 2.43%. Found: C, 45.72; H, 2.24%.

1,4,9,9,10,10-Hexachloro-2,3,6,7-tetramethyl-9,10-dihydroanthracene (5c): 44% yield from **3c**; a white solid; mp 139 °C (decomp); ^{1}H NMR δ=2.37 (s, 6H, CH_3), 2.58 (s, 6H, CH_3), and 7.73 (s, 2H, ArH); IR 750 cm^{-1} (C–Cl); MS *m/z* 440 (M^+) with an isotopic pattern of hexachlorine. Anal. Calcd for $C_{18}H_{14}Cl_6$: C, 48.80; H, 3.19%. Found: C, 48.37; H, 3.00%.

1,4,9,10-Tetrachloro-2,3-dimethylanthracene (6a). A mixture of **5a** (3.8 g, 9.2 mmol), tin(II) chloride dihydrate (29.2 g), acetic acid (40 cm³), and concd hydrochloric acid (36 cm³) was refluxed for 1.5 h. After cooling, the resulting yellow solid of **6a** was collected by filtration, washed, and purified by column chromatography on active alumina using

benzene as eluent (2.4 g, 75%). An analytical sample was obtained as yellow needles by recrystallization from chloroform–hexane; mp 119—120 °C (decomp); ^{1}H NMR δ=2.56 (s, 6H, CH_3), 7.52 (AA'BB' m, 2H, ArH), and 8.45 (AA'BB' m, 2H, ArH); IR 660 cm^{-1} (C–Cl); MS m/z 344 (M^+) with an isotopic pattern of tetrachlorine. Anal. Calcd for $C_{16}H_{10}Cl_4$: C, 55.85; H, 2.93%. Found: C, 55.84; H, 2.89%.

1,4,9,10-Tetrachloro-6,7-dimethylanthracene (6b): 80% yield; yellow needles from chloroform–hexane; mp 172 °C; ^{1}H NMR δ=2.48 (s, 6H, CH_3), 7.32 (s, 2H, ArH), and 8.45 (s, 2H, ArH); IR 810 and 605 cm^{-1}; MS m/z 344 (M^+) with an isotopic pattern of tetrachlorine. Anal. Calcd for $C_{16}H_{10}Cl_4$: C, 55.85; H, 2.93%. Found: C, 55.82; H, 3.06%.

1,4,9,10-Tetrachloro-2,3,6,7-tetramethylanthracene (6c): 75% yield; yellow needles from benzene; mp 187—188.5 °C; ^{1}H NMR δ=2.47 (s, 6H, CH_3), 2.53 (s, 6H, CH_3), and 8.23 (s, 2H, ArH); IR 670 cm^{-1} (C–Cl); MS m/z 370 (M^+) with an isotopic pattern of tetrachlorine. Anal. Calcd for $C_{18}H_{14}Cl_4$: C, 58.10; H, 3.79%. Found: C, 58.07; H, 3.58%.

3,4-Dimethylanthra[1,9-*cd*:4,10-*c'd'*]dithiole (2,3-DMTTA). In a nitrogen atmosphere, sodium metal (165 mg, 7.2 mmol) was allowed to react with sulfur (236 mg, 7.2 mmol) in dry DMF (30 cm^3) at 100 °C for 2 h, forming fresh sodium disulfide. Into the mixture was added a solution of **6a** (516 mg, 1.5 mmol) in dry DMF (30 cm^3). It was refluxed for 8 h, stirred overnight at room temperature with exposure to air, and then poured into brine (200 cm^3). The resulting brown solid was collected by filtration, dried, and extracted with hexane and then with carbon disulfide by use of a Soxhlet apparatus. The carbon disulfide extract was recrystallized from benzene to give black purple needles of 2,3-DMTTA (211 mg, 43%); mp 271 °C; IR 1610, 1300, and 740 cm^{-1}; MS m/z 330 (M^+); UV (CS_2) 450.5 (log ε 3.79), 531 (3.87), and 566.5 nm (3.90). Anal. Calcd for $C_{16}H_{10}S_4$: C, 58.15; H, 3.05%. Found: C, 58.41; H, 2.87%.

3,4-Dimethylanthra[1,9-*cd*:4,10-*c'd'*]diselenole (2,3-DMTSA). 2,3-DMTSA was prepared from a similar reaction of **6a** with sodium diselenide at 150 °C and recrystallized from benzene to give black crystals. The elemental analysis and X-ray crystallographic analysis showed that it consists of 2,3-DMTSA and benzene of 2:1 ratio. Its heating at 150 °C under a reduced pressure left the free 2,3-DMTSA: 31% yield; mp 289 °C; IR 1270 and 740 cm^{-1}; MS m/z 520 (M^+); UV (CS_2) 439.5 (log ε 3.75) and 568.5 nm (4.09). Anal. Calcd for $C_{16}H_{10}Se_4$: C, 37.09; H, 1.95%. Found: C, 37.21; H, 1.93%.

3,4-Dimethylanthra[1,9-*cd*:4,10-*c'd'*]ditellurole (2,3-DMTTeA). 2,3-DMTTeA was prepared from a similar reaction of **6a** with sodium ditelluride at 100 °C. Recrystallization from chlorobenzene gave black needles; 15% yield; mp >300 °C; IR 1250 cm^{-1}; MS m/z 714 (M^+); UV (CS_2) 598.5 nm (log ε 4.05). Anal. Calcd for $C_{16}H_{10}Te_4$; C, 26.97; H, 1.41%. Found: C, 26.96; H, 1.40%.

8,9-Dimethylanthra[1,9-*cd*:4,10-*c'd'*]dithiole (6,7-DMTTA): 2% yield; black purple powder from benzen mp >300 °C; IR 1340, 1290, 1165, and 790 cm^{-1}; MS m/z 330 (M^+); UV (CS_2) 451 (log ε 3.66), 529 (3.92), and 562 nm (3.98). Anal. Calcd for $C_{16}H_{10}S_4$: C, 58.14; H, 3.05%. Found: C, 58.08; H, 3.04%.

8,9-Dimethylanthra[1,9-*cd*:4,10-*c'd'*]diselenole (6,7-DMTSA): 38% yield; black plates from chlorobenzene; mp >300 °C; IR 1320, 1280, 1150, and 795 cm^{-1}; MS m/z 520 (M^+); UV (CS_2) 446.5 (log ε 3.66) and 568.5 nm (4.10). Anal. Calcd for $C_{16}H_{10}Se_4$: C, 37.09; H, 1.95%. Found: C, 37.19; H, 1.95%.

3,4,8,9-Tetramethylanthra[1,9-*cd*:4,10-*c'd'*]dithiole (TMTTA): 41% yield; black needles from chlorobenzene; mp >300 °C; IR 2990, 2850, and 1310 cm^{-1}; MS m/z 358 (M^+); UV (CS_2) 447.5 (log ε 3.82), 525.5 (3.89), and 557 nm (3.94). Anal. Calcd for $C_{18}H_{14}S_4$: C, 60.29; H, 3.94%. Found: C, 60.23; H, 3.85%.

3,4,8,9-Tetramethylanthra[1,9-*cd*:4,10-*c'd'*]diselenole (TMTSA): 29% yield; black powder from gradient sublimation; mp >300 °C; IR 3000, 2930, and 1290 cm^{-1}; MS m/z 548 (M^+); UV (CS_2) 559 nm (log ε 4.11). Anal. Calcd for $C_{18}H_{14}Se_4$: C, 39.59; H, 2.58%. Found: C, 39.55; H, 2.51%.

3,4,8,9-Tetramethylanthra[1,9-*cd*:4,10-*c'd'*]ditellurole (TMTTeA): 14% yield; black powder from carbon disulfide; mp >300 °C; MS m/z 740 (M^+); UV (CS_2) 586.5 nm (log ε 4.07). Anal. Calcd for $C_{18}H_{14}Te_4$: C, 29.19; H, 1.91%. Found: C, 29.48; H, 1.82%.

Charge-Transfer Complexes. All of the complexes described in this report were prepared by mixing two hot saturated solutions of the donor and acceptor in chlorobenzene. The resulting complexes precipitated out upon cooling, which were collected by filtration, washed with cold dichloromethane, and dried.

Crystal Structures. The X-ray diffraction data were collected with a Rigaku automated diffractometer using Cu $K\alpha$ radiation monochromatized with a graphite plate. Independent reflections within 2θ=126° ($|F_o| \geqslant 3.0\sigma(F_o)$) were used for analyses. The structures were solved by a direct method combined with the Monte-Carlo method for the selection of the initial set of phase,[17] and refined by a full-matrix least squares method.[18] Atomic scattering factors were taken from International Tables for X-ray Crystallography.[19] The anisotropic temperature factors were used for the refinement; hydrogen atoms were not included in the refinement. Tables of final atomic parameters, structure factors, and anisotropic thermal parameters are deposited as Document No. 9116 at the Office of the Editor of Bull. Chem. Soc. Jpn.

The present work was in part supported by the Grant-in-aid of Scientific Research on Priority Areas No. 02230222 from the Ministry of Education, Science and Culture. The authors thank Dr. K. Kawabata and Dr. M. Mizutani of Central Research Laboratories, Idemitsu Kosan Co., Ltd. for helpful discussions.

References

1) For an excellent review on TTT and TST, see I. F. Shchegolev and E. B. Yagubskii, "Extended Linear Chain Compounds," ed by J. S. Miller, Plenum Press, New York (1982), Vol. 2, pp. 385—434.

2) D. J. Sandman and J. C. Stark, *Organomet.*, **1**, 739 (1982).

3) S. Ohnishi, T. Nogami, and H. Mikawa, *Tetrahedron Lett.*, **1983**, 2401; T. Nogami, H. Tanaka, S. Ohnishi, Y. Tasaka, and H. Mikawa, *Bull. Chem. Soc. Jpn.*, **57**, 22 (1983).

4) F. Wudl, D. E. Schafer, and B. Miller, *J. Am. Chem. Soc.*, **98**, 252 (1976).

5) S. Ohnishi, T. Nogami, and H. Mikawa, *Chem. Lett.*, **1982**, 1841.

6) A. Yamahira, T. Nogami, and H. Mikawa, *J. Chem. Soc.*,

Chem. Commun., **1983**, 904; J. C. Stark, R. Reed, L. A. Acampora, D. J. Sandman, S. Jansen, M. T. Jones, and B. M. Foxman, *Organomet.*, **3**, 732 (1984).

7) T. Otsubo, N. Sukenobe, Y. Aso, and F. Ogura, *Chem. Lett.*, **1987**, 315; *Synth. Met.*, **27**, B509 (1988).

8) A preliminary account on a part of the present work has appeared: K. Takimiya, H. Miyamoto, Y. Aso, T. Otsubo, and F. Ogura, *Chem. Lett.*, **1990**, 567.

9) F. A. J. Kerdesky and M. P. Cava, *J. Am. Chem. Soc.*, **100**, 3635 (1978); F. A. J. Kerdesky, R. J. Ardecky, M. V. Lakshmikantham, and M. P. Cava, *ibid.*, **103**, 1992 (1981).

10) K. Yui, Y. Aso, T. Otsubo, and F. Ogura, *Bull. Chem. Soc. Jpn.*, **62**, 1539 (1989).

11) K. Yui, Y. Aso, T. Otsubo, and F. Ogura, *Chem. Lett.*, **1988**, 1179.

12) J. B. Torrance, *Acc. Chem. Res.*, **12**, 79 (1979); G. Saito and J. P. Ferraris, *Bull. Chem. Soc. Jpn.*, **53**, 2141 (1980).

13) J. B. Torrance, B. A. Scott, and F. B. Kaufman, *Solid State Commun.*, **17**, 1369 (1975); J. Tanaka, M. Tanaka, T. Kawai, T. Takabe, and O. Maki, *Bull. Chem. Soc. Jpn.*, **49**, 2358 (1976); E. M. Engler, V. V. Patel, J. R. Andersen, R. R. Schumaker, and A. A.Fukushima, *J. Am. Chem. Soc.*, **100**, 3769 (1978); K. Nakasuji and I. Murata, *Synth. Met.*, **27**, B289 (1988).

14) J. S. Chappell, A. N. Bloch, W. A. Bryden, M. Maxfield, T. O. Poehler, and D. O. Cowan, *J. Am. Chem. Soc.*, **103**, 2442 (1981).

15) R. P. Shibaeva, "Extended Linear Chain Compounds," ed by J. S. Miller, Plenum Press, New York (1982), Vol. 2, pp. 435—467.

16) T. J. Kristenmacher, T. J. Emge, A. N. Bloch, and D. O. Cowan, *Acta Crystallogr., Sect. B*, **38**, 1193 (1982).

17) A. Furusaki, *Acta Crystallogr., Sect. A*, **35**, 220 (1979).

18) C. Katayama, N. Sakabe, and K. Sakabe, *Acta Crystallogr., Sect. A*, **28**, S207 (1972).

19) "International Tables for X-ray Crystallography," Kynoch Press, Birmingham, England (1974), Vol. IV.